



Universiteit  
Leiden  
The Netherlands

## Metabolic and functional evaluation of diabetic cardiomyopathy using MR Spectroscopy and MR Imaging

Bizino, M.B.

### Citation

Bizino, M. B. (2022, November 16). *Metabolic and functional evaluation of diabetic cardiomyopathy using MR Spectroscopy and MR Imaging*. Retrieved from <https://hdl.handle.net/1887/3486006>

Version: Publisher's Version

License: [Licence agreement concerning inclusion of doctoral thesis in the Institutional Repository of the University of Leiden](#)

Downloaded from: <https://hdl.handle.net/1887/3486006>

**Note:** To cite this publication please use the final published version (if applicable).



# Chapter 3

## Improved Cardiac Proton Magnetic Resonance Spectroscopy at 3 T Using High Permittivity Pads

de Heer P, Bizino MB, Versluis MJ, Webb AG, Lamb HJ.

*Invest Radiol.* 2016 Feb;51(2):134-8.

## **Abstract**

### ***Objective***

The aim of this study was to determine whether high permittivity (HP) pads can be used to increase the signal-to-noise ratio (SNR) of cardiac proton magnetic resonance spectroscopy at 3 T, allowing faster data acquisition.

### ***Materials and methods***

The institutional review board approved the study protocol, and written informed consent was obtained from all participants. In 22 healthy volunteers, water-suppressed localized spectra were acquired in the interventricular septum without and with HP pads. The SNR and myocardial triglyceride content (MTGC) were measured without and with the HP pads, and the results were compared with a paired sample Student t test.

### ***Results***

Application of HP pads increased mean (SD) SNR from 27.9 (15.6) to 42.3 (24.4) ( $P < 0.0001$ ), a mean gain of 60%. The acquisition time can thereby be reduced from just under 5 minutes to just under 2 minutes while maintaining the same SNR. The mean (SD) MTGC was 0.39% (0.17%) without pads and 0.38% (0.15%) with pads ( $P = 0.83$ ) for the healthy volunteers, showing that no bias is introduced by using the pads. No difference in spectral linewidth was measured ( $P = 0.80$ ), the values being 17.4 (4.9) Hz without and 17.1 (3.2) Hz with pads. Both transmit and receive maps showed increases in sensitivity due to the presence of the HP pads.

### ***Conclusions***

High permittivity pads improve cardiac proton magnetic resonance spectroscopy at 3 T by increasing the SNR on average by 60%, which can be used to reduce data acquisition time significantly, allowing fast assessment of MTGC without compromising spectral quality. The SNR increase arises primarily from the increase in receive sensitivity of the phased array, which is more closely coupled to the body via

the HP pads. In addition, the transmit efficiency is also increased, allowing shorter or lower power radiofrequency pulses.

## Introduction

Myocardial triglyceride content (MTGC) reflects the process of ectopic intracellular fat accumulation, which is linked to the development of heart failure.<sup>1</sup> This process is called steatosis and has proved to be an important parameter in the field of cardiovascular disease related to obesity, metabolic syndrome, and type 2 diabetes mellitus.<sup>2-8</sup> Myocardial steatosis can be reversed using therapeutic procedures, a fact which emphasizes the importance of a reliable measurement technique to monitor the cardiac MTGC. The criterion standard for the quantification of cardiac MTGC is proton magnetic resonance spectroscopy (<sup>1</sup>H-MRS). However, cardiac <sup>1</sup>H-MRS is challenging due to an intrinsic low signal-to-noise ratio (SNR) as well as static and dynamic fluctuations in both the main magnetic field ( $B_0$ ) as well as in the transmit field ( $B_1^+$ ). To increase the SNR, many signal averages must be coadded, often between 32 and 128 averages at a field strength of 1.5 T. This will result in long acquisition times, more than 10 minutes, limiting the use of cardiac <sup>1</sup>H-MRS in a practical clinical protocol in which many other types of scan must also be acquired. Another method to increase SNR is to acquire data at a higher field strength.<sup>9</sup> However, cardiac <sup>1</sup>H-MRS at 3 T is even more challenging than at 1.5 T due to increases in the degree of static and dynamic  $B_0$  and  $B_1^+$  inhomogeneities. Dynamic  $B_0$  fluctuations, caused mainly by respiratory motion, result in phase and frequency variations between consecutive signal averages, thereby decreasing signal intensity and increasing linewidths (as well as changing line shape from Gaussian to Voigt) and complicating MTGC quantification. Dynamic  $B_1^+$  inhomogeneities, caused also by respiratory motion, result in fluctuations in signal intensity per signal average.

Recent work has shown that it is possible to increase the quality of 3 T cardiac imaging, simultaneously increasing  $B_1^+$  homogeneity over the volume of interest (VOI) and decreasing the required power, using high permittivity (HP) pads.<sup>10</sup> Therefore, the purpose of this study was to determine whether the application of HP pads can increase the SNR in cardiac <sup>1</sup>H-MRS at 3 T, allowing shorter data acquisition times.

## Materials and methods

### *Participants*

The institutional review board approved the study protocol, and written informed consent was obtained from all participants. The study was conducted according to the principles expressed in the Declaration of Helsinki. Twenty-two healthy volunteers underwent cardiac  $^1\text{H}$ -MRS from December 2013 until February 2014. Because of a voxel placement error (contamination with pericardial lipid), 2 volunteers were excluded from further analysis. The remaining 20 volunteers consisted of 12 female and 8 male subjects with a mean (SD) age of 29 (11) years (range, 19–53 years) and with a mean (SD) body mass index of 23 (3)  $\text{kg}/\text{m}^2$  (range, 19.7–34.1  $\text{kg}/\text{m}^2$ ).

### *Data acquisition*

Experiments were performed on a 3 T Ingenia whole-body magnetic resonance imaging scanner (Philips Healthcare, Best, the Netherlands) with dual-channel transmit capability. The body coil was used for transmission and an anterior (16 elements) and posterior (12 elements) array for reception. The entire scan protocol was performed twice: once without the HP pads and once with the HP pads placed between the patient and the receive array on the anterior and posterior sides of the thorax. To reduce any potential confounding factors, such as the duration that the volunteer had to lie in the magnet, data were acquired with a random choice of which configuration was used first. Proper placement of the pads was confirmed by a 30-second survey scan. A series of scout scans was performed to localize the MRS voxel, 15 mL ( $40 \times 15 \times 25 \text{ mm}^3$ ), within the myocardial interventricular septum (Fig. 1A). Point resolved spectroscopy spectra<sup>11</sup> were acquired with an echo time of 35 milliseconds without water suppression (repetition time: 9 seconds, 16 averages) and with selective excitation water suppression (repetition time: 3.5 seconds, 12–48 averages).

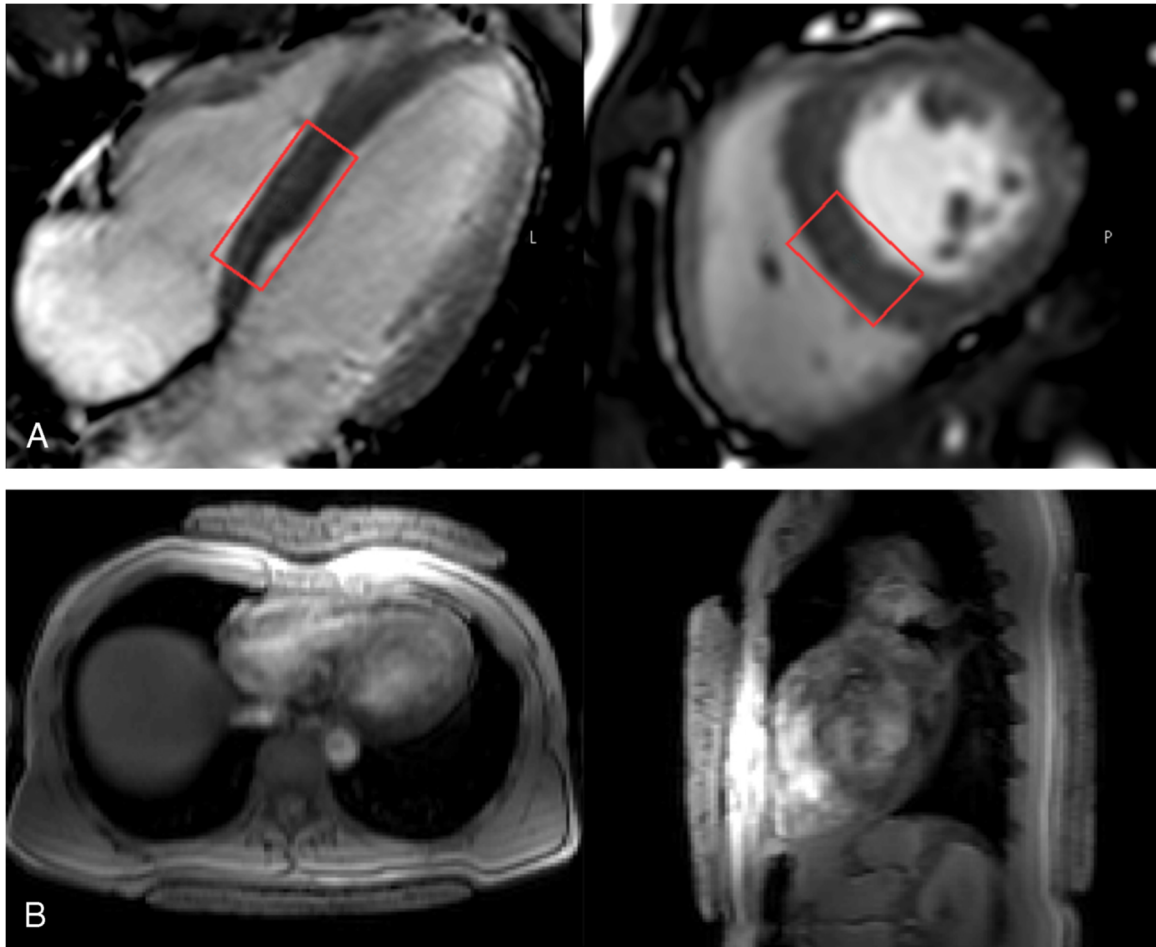


**Figure 1.** A, Placement of the spectroscopy voxel (red box) in the interventricular septum on the 4-chamber and short axis view. B, Placement of the HP pads shown on the transverse and sagittal survey scan. Both the anterior and posterior HP pads were entered on the location of the spectroscopy VOI in both the feet-head and left-right direction. Figure 1 can be viewed online in color at [www.investigativeradiology.com](http://www.investigativeradiology.com).

The unsuppressed spectrum was used as a reference for triglyceride quantification. Before each scan radiofrequency (RF) pulse power optimization, pencil beam B0 shimming and resonance frequency determination were performed using 5 breath-holds (exhalation). All spectral acquisitions were respiratory navigator gated.<sup>12</sup> With a mean (SD) navigator efficiency of 57% (10%), this resulted in a mean acquisition time of 4 minutes and 55 seconds for the water-suppressed spectra (48 averages). The preparation time was on average 1 minute and 56 seconds, and the acquisition of the reference signal was 4 minutes and 15 seconds, resulting in a mean total scan time of 11 minutes and 6 seconds. Individual signal averages were saved separately for subsequent data processing. The navigator axis was placed along the lung-liver interface. Measurements were performed to determine the most stable cardiac phase

for the electro-cardiographical triggering delay and resulted in a post R-wave delay of 200 to 250 milliseconds, depending on the heart rate, which agrees with results from previous authors.<sup>13</sup>

For 11 volunteers, transmit field ( $B_1^+$ ) maps were measured based on the saturated double-angle method.<sup>14</sup> Reception sensitivity ( $B_1^-$ ) maps were calculated in 4 volunteers. This was done by acquiring electrocardiography-triggered 3-dimensional (3D) gradient-echo sequence with a flip angle of 5 degrees, geometrically aligned with the  $B_1^+$  map. The resulting image is proportional to the product of the receive sensitivity and the  $B_1^+$ , as described by Wang et al.<sup>15</sup> The receive sensitivity is then calculated by dividing the 3D gradient-echo image by the  $B_1^+$ .

### ***Preparation of HP pads***

The HP pads were constructed using an aqueous ( $H_2O$ ) suspension of barium titanate with a 4:1 mass-mass ratio.<sup>10</sup> This results in a very dense mixture with a relative permittivity of approximately 300. Two HP pads, one 2-cm thick (placed anterior) and the other 1-cm thick (placed posterior), with a dimension of 20 x 20  $cm^2$  were respectively centered above and below the location of the spectroscopy VOI in both the feet-head and left-right direction (Fig. 1B). The weights of these HP pads were 2.3 kg and 1.3 kg, respectively.

### ***Data processing***

The spectra were fitted in the time domain to a Gaussian line shape using the advanced method for accurate, robust, and efficient spectral fitting algorithm in Java-Based Magnetic Resonance User Interface (jMRUI v5.0; MRUI Project).<sup>16</sup> As prior knowledge, the linewidth of the  $CH_3$  resonance was set to be equal to that of the  $(CH_2)_n$  groups, and the frequency of the  $CH_3$  peak was fixed at  $-0.4$  ppm with respect to the frequency of the  $(CH_2)_n$  peak. The SNR is defined as the summed amplitude of the spectral component of the triglyceride-methyl ( $CH_3$ ) and the triglyceride-methylene  $(CH_2)_n$  peaks divided by the SD of the noise. The noise was taken from the last 100 data points of the time-domain free induction decay, which was confirmed to be signal free. The total MTGC was calculated using the equation 1:



$$\frac{\text{triglyceride methyl (CH}_3\text{)} + \text{triglyceride methylene (CH}_2\text{)}^n}{\text{water} + \text{triglyceride methyl (CH}_3\text{)} + \text{triglyceride methylene (CH}_2\text{)}^n} \times 100\%$$

The SNR for reduced scan times was calculated for 48 to 36, 24, and 12 averages, reducing the mean acquisition times from 5 to 3.75, 2.5, and 1.25 minutes, respectively, to study the effect of scan time on SNR without and with pads. To test the effect of the HP pads on the linewidth, the full width at half maximum of the water peak was measured in all volunteers. The average transmit power values from the RF amplifier were read from the log file produced by the scanner.

### ***Statistical analysis***

All statistical analyses were performed by using statistical software IBM SPSS Statistics (version 20, IBM, Chicago, IL). Numerical data were reported as mean (SD). A paired samples Student *t* test was performed to compare SNR, spectral linewidths, fat fraction, and RF transmit power without and with the HP pads. Data were considered statistically significant at *P* values less than 0.05. measured in all volunteers. The average transmit power values from the RF amplifier were read from the log file produced by the scanner.

## **Results**

### ***Signal-to-noise ratio***

Three different spectra from a single volunteer are shown in Figure 2. The SNR is increased by 90% for this volunteer by applying the HP pads, as shown by comparing the middle and left spectra. A comparison of the middle and right spectra shows that the same spectral SNR can be achieved using the pads with 60% fewer signal averages.

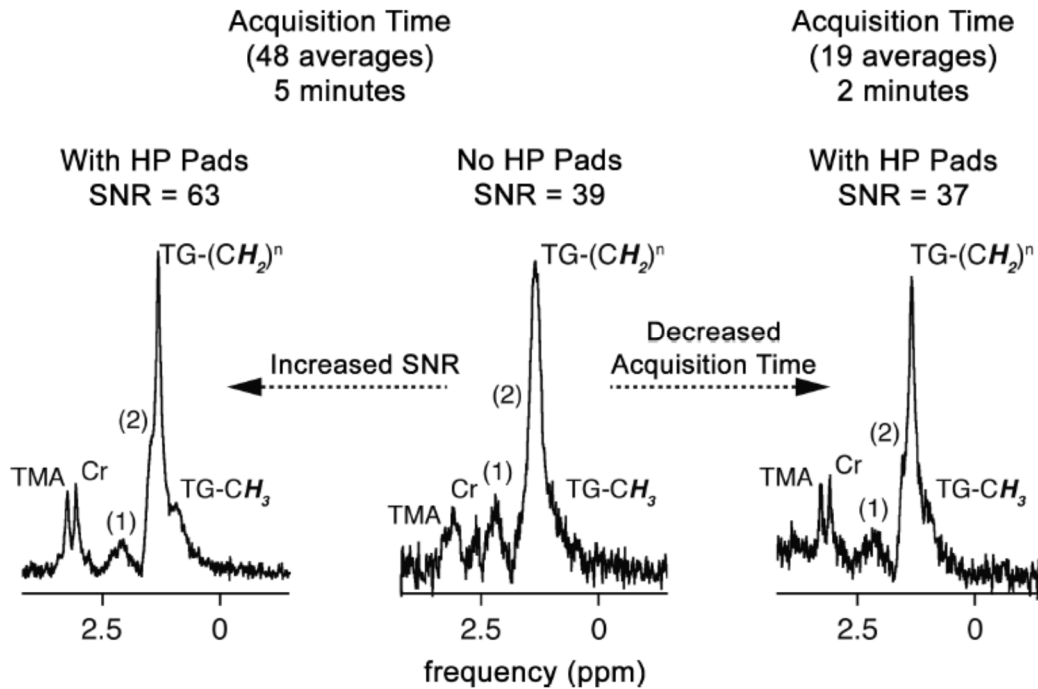


**Figure 2.** Three water-suppressed spectra of a single volunteer. The spectrum on the left was acquired with the HP pads, and the spectrum in the center was acquired without the pads in place. The spectrum on the right is identical to the left spectrum (with HP pads) but has been reconstructed with only the first 19 averages of the total 48 averages. Multiple triglyceride resonances [ $\text{CH}_3$  at 0.9 ppm,  $(\text{CH}_2)_n$  at 1.3 ppm,  $\text{CH}_2\text{CH}_2\text{COO}$  marked with number 2 at 1.5 ppm,  $\text{CH}_2\text{CH}=\text{CHCH}_2$  and  $\text{CH}_2\text{COO}$  marked with number 1 around 2.1 ppm], a creatine methyl resonance at 3.0 ppm, and a trimethylammonium resonance at 3.2 ppm can be distinguished in the spectrum.

In Figure 3, the MTG SNR is plotted for each volunteer without and with HP pads. The mean (SD) SNR increased from 27.9 (15.6) to 42.3 (24.4) ( $P < 0.0001$ ), and the SNR change ranged from  $-4.0$  to  $+44.0$  with an average increase of 14.2. The mean gain in SNR by using the HP pads is 60%. Measurements of the noise showed a significant increase with the pads in place ( $3.36 \times 10^{-6}$  [8.04] without,  $4.06 \times 10^{-6}$  [9] and with pads), implying a closer coupling to the region of interest, resulting in an overall increase in SNR.

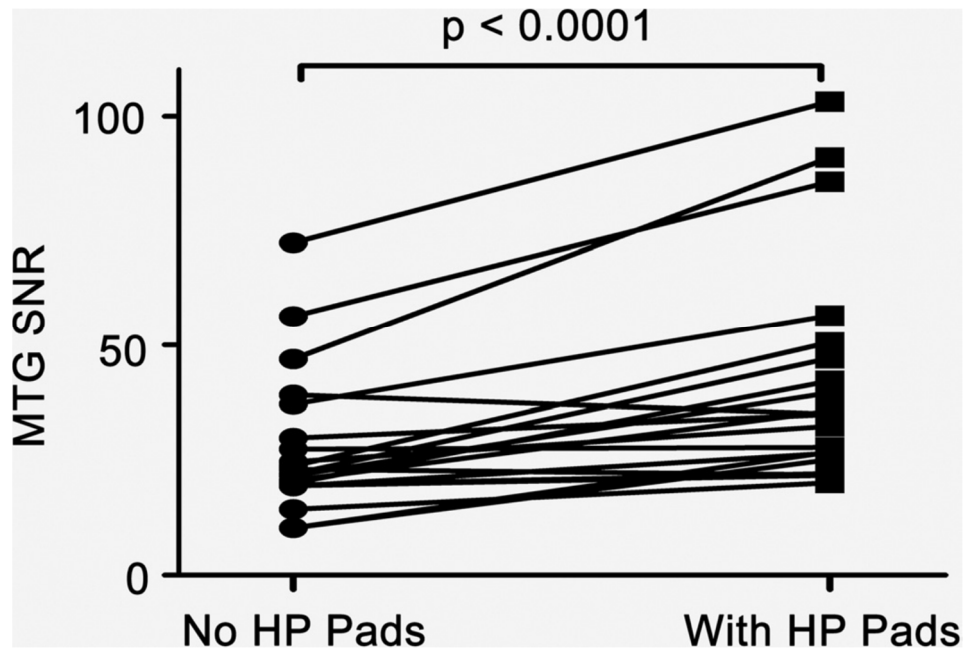


Figure 3. Myocardial triglyceride SNR without and with the HP pads (48 averages).

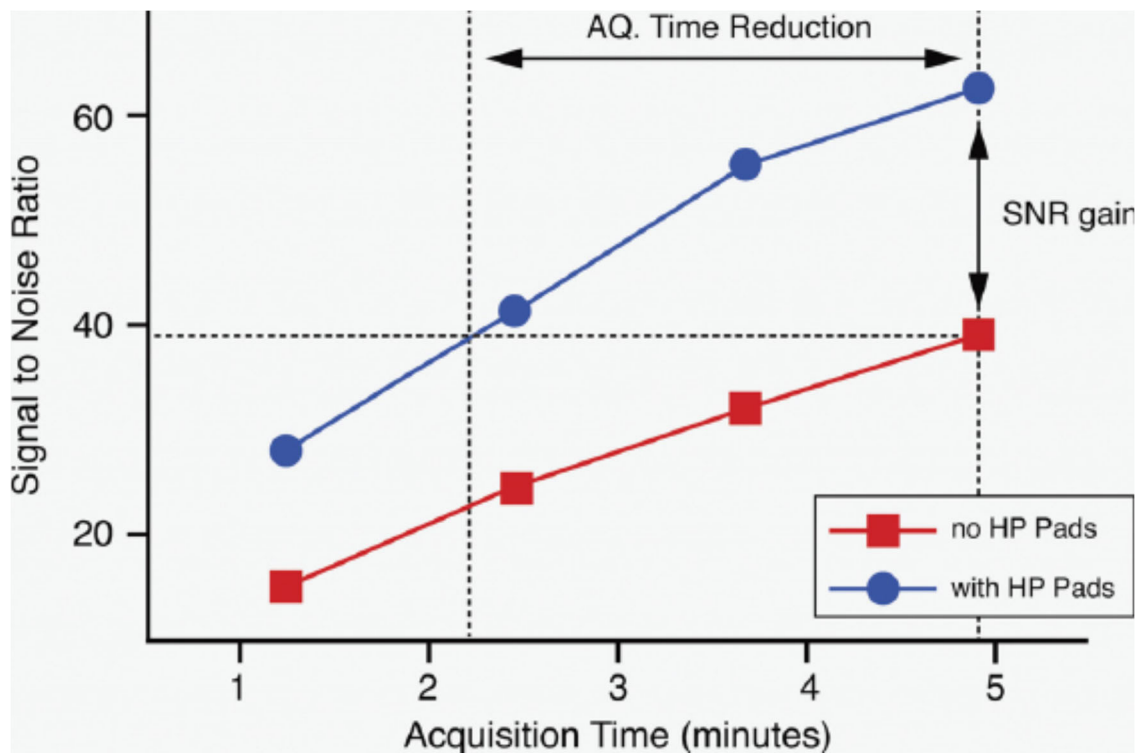


Figure 4. Signal-to-noise ratio of the MTG signal against acquisition time, acquired in the same volunteer as shown in Figure 2, without and with the HP pads. The horizontal dotted line is the SNR level of the total acquisition (5 minutes) without the HP pads. This plot shows the SNR of the full scan without pads is reached in just over 2 minutes when using the HP pads effectively cutting acquisition time more than half. Figure 4 can be viewed online in color at [www.investigativeradiology.com](http://www.investigativeradiology.com).

In Figure 4, the SNR of the MTG signal as a function of the acquisition time is shown for a single volunteer. It can be seen that significant reductions in time, for this

volunteer from 5 minutes to a just over 2 minutes (similar to the data shown in Fig. 2), can be achieved by using the HP pads while maintaining the same SNR equal compared with the scan without the HP pads.

### ***Linewidth***

There was no significant difference ( $P = 0.80$ ) in the linewidths without and with the HP pads, the values being 17.4 (4.9) Hz and 17.1 (3.2) Hz, respectively.

### ***Transmit and receive sensitivities***

The peak  $B_1^+$  available on the scanner is 13.5  $\mu\text{T}$ . Without the HP pads, the transmit field strength in the VOI was 11.2 (1.4)  $\mu\text{T}$ , whereas with the pads, a transmit field of 12.5 (1.3)  $\mu\text{T}$  was reached ( $P = 0.0001$ ). This translates to an average increase in  $B_1^+$  of 12% in the VOI. The average required power for the scan was 20.9 W without the HP pads and 17.1 W with the HP pads ( $P < 0.0001$ ).

The receive sensitivity ( $B_1^-$ ) increased from 326 (50) without the HP pads to 424 (45) with the HP pads. This translates to an average increase in  $B_1^-$  of 30% in the VOI. Figure 5A shows transmit ( $B_1^+$ ) fields per square root of input power in a single volunteer without and with the HP pads. The field is plotted along the long axis of the selected volume shown in Figure 1. Figure 5B shows the corresponding  $B_1^+$  field achieved with the slice-selective power optimization on the scanner, and Figure 5C shows the calculated receive sensitivity ( $B_1^-$ ) maps.

### ***Myocardial triglyceride content***

The MTGC was calculated to be 0.39% (0.17%) without the HP pads and 0.38% (0.15%) with the HP pads ( $P = 0.83$ ).

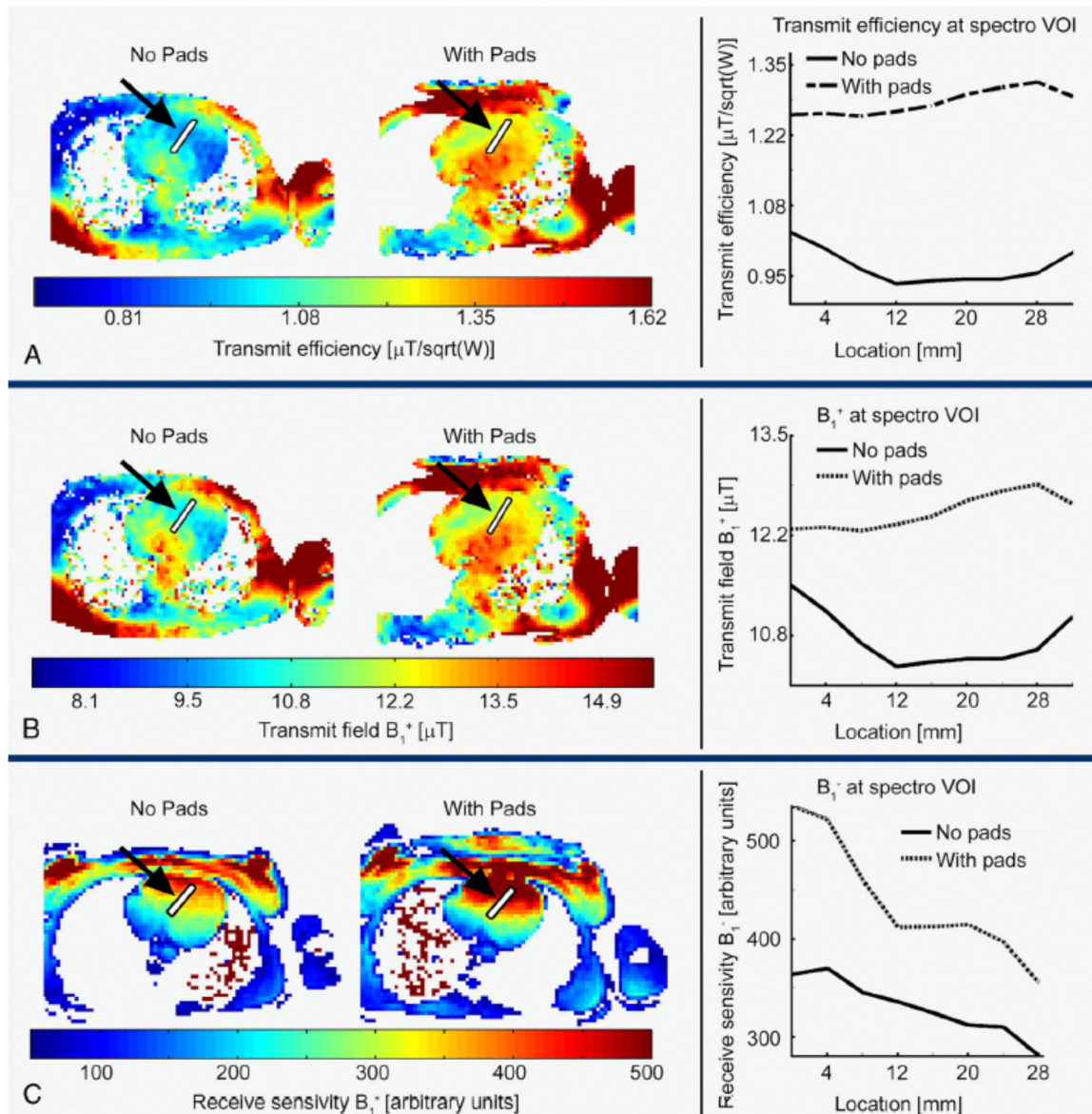


**Figure 5.** A, On the left the  $B_1^+$  maps are shown for a single volunteer without and with the HP pads. The gain in SNR was 40% for this volunteer. The maximum transmit field from the body coil is set at 13.5  $\mu\text{T}$ . On the right, the  $B_1^+$  intensity is plotted at the location of the spectroscopy voxel that is noted as a white line from anterior to posterior in the  $B_1^+$  maps. B, The left panel shows  $B_1^-$  maps of a single volunteer without and with the HP pads placed. The gain in SNR was 110% for this volunteer. In the right panel,  $B_1^-$  intensity is plotted at the location of the voxel of interest that is noted as a white line from anterior to posterior in the  $B_1^-$  maps. Figure 5 can be viewed online in color at [www.investigativeradiology.com](http://www.investigativeradiology.com).

## Discussion

The main finding of this study is that the HP pads significantly increase the SNR of cardiac  $^1\text{H}$ -MRS at 3 T. The increased SNR can be exploited to reduce the number of required signal averages, reducing the mean acquisition time by 60%. The acquisition time for our standard MRS protocol can in this way be reduced from 5 minutes to only

2 minutes for the same spectral quality. These results are in line with a previous study on the effects of HP pads on cardiac imaging,<sup>10</sup> although in that particular study quantitative analysis was performed across the entire cardiac volume, rather than the much smaller section of the myocardial wall from which spectra were acquired in this study. The authors found significant increases in receive sensitivity close to the anterior section of the heart, with Figure 5 displaying an approximately 30% increase in receive sensitivity, very similar to that quantitatively determined in this current study.

Our results show that the main factor responsible for the increased SNR is the 30% increase in receive sensitivity due to an increased coupling between the coil array and the body by using the HP pads. The transmit field increased by 12% on average accompanied by an 18% decrease in average power resulting in a significantly increased transmit efficiency. This effect was also seen in a previous study, which considered the effects of the HP pads in cardiac imaging.<sup>10</sup> No significant differences in spectral linewidth were measured using the HP pads, which can be explained by the large distance between HP pads and the VOI. From the SNR results for all volunteers, it was noted that, in 2 of the total 20 volunteers, adding the pads decreased the SNR. This did not seem to be related to body size or sex and is most likely related to faulty placement of the pads. We also observed a large variance in spectral SNR between the different volunteers. This variance did not seem to be correlated with body mass index but more likely to the chest size and subcutaneous fat levels. Although volunteers noted the extra weight of the HP pad in addition to that of the receive array on their chest, they did not rate this as uncomfortable. The effect on the SAR of the HP pads has been described previously in the study by Brink and Webb<sup>10</sup> (Fig. 3). They showed that the local increase in transmit efficiency resulted in lower input power being required to produce a given transmit field, which therefore reduced the local SAR throughout the body.

Despite the clear increase in SNR afforded by the use of the HP pads, it is important that their use does not introduce a measurement bias into the MTGC quantification. Our results showed statistically identical values without (0.39%

[0.17%]) and with (0.38% [0.15%]) the HP pads ( $P = 0.83$ ), meaning that lipid quantification is not affected by using the pads. The MTGC for the healthy volunteers was in agreement with previous studies.<sup>17–19</sup>

In conclusion, HP pads improve cardiac  $^1\text{H}$ -MRS at 3 T by increasing the SNR on average by 60%, which can be used to reduce data acquisition time, significantly allowing fast assessment of MTGC without compromising spectral quality. The same pads as the Brink and Webb (MRM 2014) study were used for this study. This set of pads was optimized to “maximize the average transmit efficiency and to minimize the  $B_1$  inhomogeneity (s), over the entire 3D heart volume”. As such, there may be some improvements that could be made because we are interested in a relatively small subsection of the heart for spectroscopy.

## References

1. Bizino MB, Hammer S, Lamb HJ. Metabolic imaging of the human heart: clinical application of magnetic resonance spectroscopy. *Heart*. 2014;100:881–890.
2. Bottomley PA, Weiss RG. Non-invasive magnetic-resonance detection of creatine depletion in non-viable infarcted myocardium. *Lancet*. 1998;351:714–718.
3. Kankaanpää M, Lehto HR, Pärkkä JP, et al. Myocardial triglyceride content and epicardial fat mass in human obesity: relationship to left ventricular function and serum free fatty acid levels. *J Clin Endocrinol Metab*. 2006;91:4689–4695.
4. McGavock JM, Lingvay I, Zib I, et al. Cardiac steatosis in diabetes mellitus: a <sup>1</sup>H-magnetic resonance spectroscopy study. *Circulation*. 2007;116:1170–1175.
5. Nakae I, Mitsunami K, Omura T, et al. Proton magnetic resonance spectroscopy can detect creatine depletion associated with the progression of heart failure in cardiomyopathy. *J Am Coll Cardiol*. 2003;42:1587–1593.
6. Reingold JS, McGavock JM, Kaka S, et al. Determination of triglyceride in the human myocardium by magnetic resonance spectroscopy: reproducibility and sensitivity of the method. *Am J Physiol Endocrinol Metab*. 2005;289:E935–E939.
7. Szczepaniak LS, Dobbins RL, Metzger GJ, et al. Myocardial triglycerides and systolic function in humans: in vivo evaluation by localized proton spectroscopy and cardiac imaging. *Magn Reson Med*. 2003;49:417–423.
8. van der Meer RW, Doornbos J, Kozerke S, et al. Metabolic imaging of myocardial triglyceride content: reproducibility of <sup>1</sup>H MR spectroscopy with respiratory navigator gating in volunteers. *Radiology*. 2007;245:251–257.
9. Stephenson MC, Gunner F, Napolitano A, et al. Applications of multi-nuclear magnetic resonance spectroscopy at 7T. *World J Radiol*. 2011;3:105–113.
10. Brink WM, Webb AG. High permittivity pads reduce specific absorption rate, improve B1 homogeneity, and increase contrast-to-noise ratio for functional cardiac MRI at 3 T. *Magn Reson Med*. 2014;71:1632–1640.
11. Bottomley PA. Spatial localization in NMR spectroscopy in vivo. *Ann N Y Acad Sci*. 1987;508:333–348.
12. Schär M, Kozerke S, Boesiger P. Navigator gating and volume tracking for double-triggered cardiac proton spectroscopy at 3 Tesla. *Magn Reson Med*. 2004;51:1091–1095.
13. Carlsson Åsa, Sohlin Maja, Ljungberg Maria, et al. The cardiac triggering time delay is decisive for the spectrum quality in cardiac <sup>1</sup>H MR Spectroscopy. *Proc Intl Soc Mag Reson Med*. 2012;20:1793.
14. Cunningham CH, Pauly JM, Nayak KS. Saturated double-angle method for rapid B1+ mapping. *Magn Reson Med*. 2006;55:1326–1333.
15. Wang J, Yang QX, Zhang X, et al. Polarization of the RF field in a human head at high field: a study with a quadrature surface coil at 7.0 T. *Magn Reson Med*. 2002;48:362–369.
16. Naressi A, Couturier C, Devos JM, et al. Java-based graphical user interface for the MRUI quantitation package. *MAGMA*. 2001;12:141–152.
17. Weiss K, Martini N, Boesiger P, et al. Cardiac proton spectroscopy using large coil arrays. *NMR Biomed*. 2013;26:276–284.
18. Rial B, Robson MD, Neubauer S, et al. Rapid quantification of myocardial lipid content in humans using single breath-hold <sup>1</sup>H MRS at 3 Tesla. *Magn Reson Med*. 2011;66:619–624.
19. Faller KM, Lygate CA, Neubauer S, et al. (<sup>1</sup>H)-MR spectroscopy for analysis of cardiac lipid and creatine metabolism. *Heart Fail Rev*. 2013;18:657–668.



